Efficient CM-FEM modeling of coplanar waveguides for high-speed e/o modulators

Francesco Carbonera, Francesco Bertazzi, Michele Goano, Giovanni Ghione
Dipartimento di Elettronica, Politecnico di Torino, Corso Duca degli Abruzzi 24, 10129 Italy
E-mail: ghione@polito.it

Abstract

A general approach is proposed for the accurate and efficient computation of the characteristic parameters of coplanar waveguides having electrodes of complex cross-section on multi-layered, planar or non-planar substrates, as presently considered for high-speed (semiconductor or $LiNbO_3$) electrooptic modulators. The approach is based on the coupling of quasi-TEM finite element method with numerical conformal mapping, and provides the frequency-dependent parameters of an equivalent transmission line model. The present technique, implemented in MATLAB as a practical design tool, is compared with semi-analytical methods (when applicable) and full-wave finite element method: excellent agreement is demonstrated with the full-wave solution, at a fraction of its computational cost.

1 Introduction

High-speed coplanar electrooptic (e/o) modulators on $LiNbO_3$ or other substrates (e.g. semiconductors exploiting bulk or QW e/o effects) currently exhibit bandwidths in excess of 40 GHz with on-off modulation voltages around 5 V. The design of such structures is extremely difficult because of the stringent and contrasting requirements in terms of velocity matching with the optical signal, low microwave attenuation, and good superposition between the optical and microwave fields. Moreover, complex structures with layered dielectrics, non-rectangular lines, ridged substrates are exploited for improved performance (see Fig. 1). Owing to the very narrow margins left for the optimization of coplanar e/o modulators, an accurate but efficient numerical model is mandatory to allow a systematic exploration of the parameter space in search of an optimum structure prior to technological implementation.

During the last few years, several models have been presented for coplanar waveguides in e/o modulators. Analytical or semi-analytical approaches [1] are accurate and fast but cannot deal with arbitrarily shaped metallic electrodes (e.g. mushroom, trapezoidal, or non-planar electrodes). Besides, in such models multilayered dielectric substrates are dealt with only approximately, and non-planar substrates (e.g. with grooves or ridges) are excluded. Finally, analytical models do not allow a self-consistent evaluation of the superposition integral, and therefore of the on-off voltage. Numerical models have been presented based on both quasi-TEM and full-wave approaches. Quasi-TEM models usually fail to yield an accurate approximation of conductor losses, whose investigation is basic in our case, while full-wave models, though in principle capable to simulate all of the relevant features, are often too computationally intensive to allow for structure optimization.

In the present paper, we develop a new, efficient and accurate quasi-TEM model by coupling a numerical conformal mapping technique [2] with the numerical (FEM) solution of the electrical problem. Starting from analytical or numerical approximations of the optical field, the model allows also the evaluation of the superposition integral. In order to investigate the numerical accuracy of the model, extensive comparisons are presented with the results of a full-wave vector FEM code (FW-FEM) [3] which computes the solution within the field-penetrated metallic electrodes and therefore the correct transition of the attenuation coefficient from the low-frequency to the skin-effect regime.

2 The model

The model proposed is based on the quasi-TEM approach. Owing to the extremely small line cross section (tipically gaps and line widths are of the order of 10 μm), modal dispersion is negligible up to the mm-wave range. The characterization of the quasi-TEM parameters ($\mathcal{R}$, $\mathcal{G}$, $\mathcal{C}$, $\mathcal{L}$) is carried out as follows:

- The per-unit-length capacitance with dielectrics $\mathcal{C}$ and the per-unit-length conductance $\mathcal{G}$ are numerically evaluated from Laplace's equation

$$\nabla_t \cdot (\boldsymbol{\epsilon}_r \cdot \nabla_t \phi) = 0 \tag{1}$$

  where ϕ is the electrostatic potential, and $\boldsymbol{\epsilon}_r$ is the complex permittivity tensor. In this paper, we assume that the imaginary part of the permittivity tensor $\boldsymbol{\epsilon}_r$ is expressed by a frequency-independent loss tangent. A frequency

dependent loss tangent can be accounted for, if needed, but equation (1) must then be solved for each frequency value. It is easily shown that $\mathcal{G}$ and $\mathcal{C}$ are related to the total electrostatic energy by

$$(\mathcal{G} + j\omega\mathcal{C})\, V^2 = j\omega(\boldsymbol{\phi}^\dagger \cdot \boldsymbol{K} \cdot \boldsymbol{\phi}) \tag{2}$$

$$\boldsymbol{K} = \sum_e \iint_e \left(\epsilon_{rxx}\{\boldsymbol{N}_x\} \cdot \{\boldsymbol{N}_x\}^T + \epsilon_{ryy}\{\boldsymbol{N}_y\} \cdot \{\boldsymbol{N}_y\}^T\right) \mathrm{d}x\, \mathrm{d}y \tag{3}$$

where the column vector $\boldsymbol{\phi}$ is the FEM representation of of the potential function ϕ, V is the applied voltage, and $\{\boldsymbol{N}_x\} = \partial\{\boldsymbol{N}\}/\partial x$, $\{\boldsymbol{N}_y\} = \partial\{\boldsymbol{N}\}/\partial y$ are the spatial derivatives of the conventional nodal shape function vector $\{\boldsymbol{N}\}$. The sparse matrix $\boldsymbol{K}$ is obtained assembling and integrating the local matrices $\{\boldsymbol{N}_x\} \cdot \{\boldsymbol{N}_x\}^T$ and $\{\boldsymbol{N}_y\} \cdot \{\boldsymbol{N}_y\}^T$ over each element of the computational domain. Analytical expression for these integrals are reported in [4].

- The per-unit-length resistance $\mathcal{R}$ generally depends on frequency, since it behaves asymptotically as $\sqrt{f}$ owing to the skin effect, but also saturates at low frequency to the DC value, with a complex frequency behaviour which depends on the conductors shape. In the present work, the high-frequency, skin-effect behaviour is exactly evaluated through numerical conformal mapping [5, 6] according to a novel approach which allows for arbitrarily shaped electrodes [2]. The DC value is directly estimated from the electrode cross section, and is connected to the high-frequency regime through a simple blending expression. The resulting model is accurate over a frequency interval covering all the range significant for the present application.

- The per-unit-length inductance $\mathcal{L}$ again depends on frequency due to the frequency-dependent internal inductance $\mathcal{L}_{\text{int}}$. As well known, the internal inductive reactance at high frequency equals the skin-effect resistance; this is exploited to provide the high-frequency behaviour for the internal inductance. The external contribution $\mathcal{L}_{\text{ext}}$ can be derived from the capacitance in air obtained from conformal mapping. The high-frequency and DC regimes are connected through a simple blending formula, and the DC inductance is evaluated from Poisson's equation

$$\nabla \cdot \left(\boldsymbol{\mu}_r^{-1} \cdot \nabla A\right) = -J_z \tag{4}$$

where A is the z-directed magnetostatic potential, $\boldsymbol{\mu}_r$ is the permeability tensor, and J_z is the uniform current distribution on the electrodes. The inductance $\mathcal{L}_{\text{DC}}$ is related to the magnetostatic energy by

$$\mathcal{L}_{\text{DC}}\, I^2 = \boldsymbol{A}^\dagger \cdot \boldsymbol{M} \cdot \boldsymbol{A} \tag{5}$$

$$\boldsymbol{M} = \sum_e \iint_e \left(\mu_{rxx}^{-1}\{\boldsymbol{N}_x\} \cdot \{\boldsymbol{N}_x\}^T + \mu_{ryy}^{-1}\{\boldsymbol{N}_y\} \cdot \{\boldsymbol{N}_y\}^T\right) \mathrm{d}x\, \mathrm{d}y \tag{6}$$

where $\boldsymbol{A}$ is the FEM representation of A, and I is the current carried by the active electrode.

The quasi-TEM model has been fully implemented in the MATLAB environment as a practical design tool. In summary, the proposed approach allows for RC low-frequency dispersion computations and provides a very accurate (virtually exact) model for high-frequency, skin-effect losses. Moreover, it allows the superposition integral to be directly estimated thanks to the availability of the quasi-TEM microwave field. The optical field distribution can be either derived from numerical approaches (including analytical approximations) or fitted from experimental results.

3 Validation and examples

As a first numerical example we consider a rectangular CPW on a X-Cut Y-Propagating $LiNbO_3$ substrate (the relative permittivities are 43 and 28 perpendicular and parallel to the substrate surface, respectively) and a SiO_2 buffer layer with thickness $t_{\text{b}} = 1\,\mu$m and relative permittivity $\epsilon_{r,\text{b}} = 3.90$. The gold ($\sigma = 4.1 \times 10^7$ S/m) electrode thickness is $t = 10\,\mu$m. The central electrode width is $W = 15\,\mu$m, and the spacing between the line and the ground planes is $G = 10\,\mu$m. The loss tangent values used in all computations are $\tan\delta_{\text{s}} = 0.005$ for the $LiNbO_3$ substrate, and $\tan\delta_{\text{b}} = 0.026$ for the SiO_2 buffer layer. Adaptive grid refinement is exploited to increase the solution accuracy near edge singularities. Moreover, properly dense meshes are adopted in correspondence of the optical waveguides, in order to increase the accuracy of the superposition integral (see Fig. 3). Fig. 4 shows a comparison between the per-unit-length inductance computed with FW-FEM, the present approach (CM-FEM), and the quasi-TEM analytical model proposed in [7] for thick rectangular waveguides as extended in [1] to oxide-covered substrates. The agreement is very good for all models, with the exception of a transition region well below the frequency range of interest for high-speed modulation. In Fig. 5, the microwave

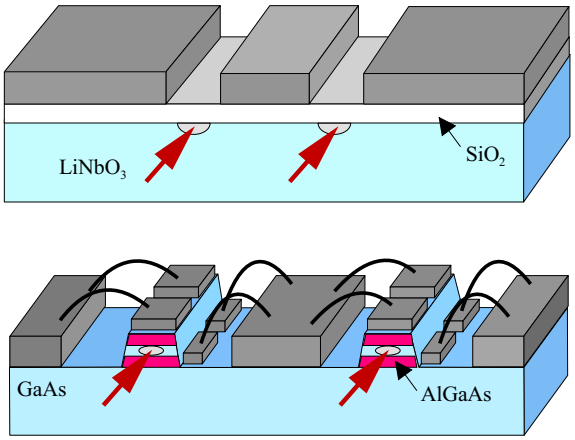

Figure 1: Cross-sections of some line geometries proposed for high-speed e/o modulators on $LiNbO_3$ (above) or semiconductor (below) substrates.

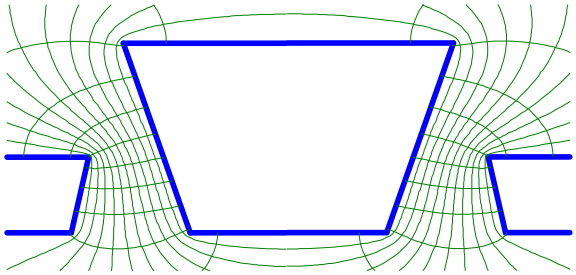

Figure 2: Potential distribution in air obtained with numerical CM for a trapezoidal CPW.

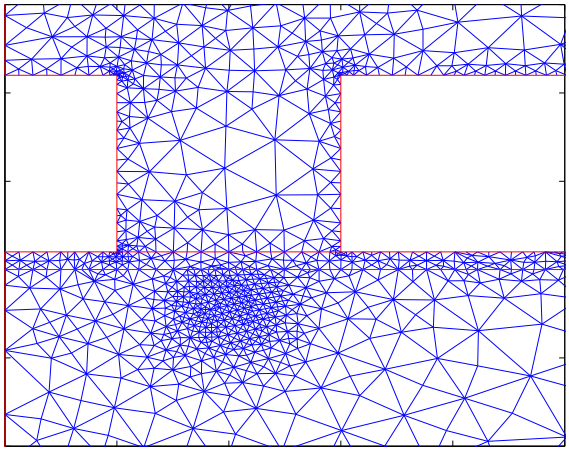

Figure 3: Detail of the quasi-TEM FEM mesh for a modulator with rectangular electrodes, showing the denser regions in correspondence of the line edges, the thin oxide layer, and the optical waveguide.

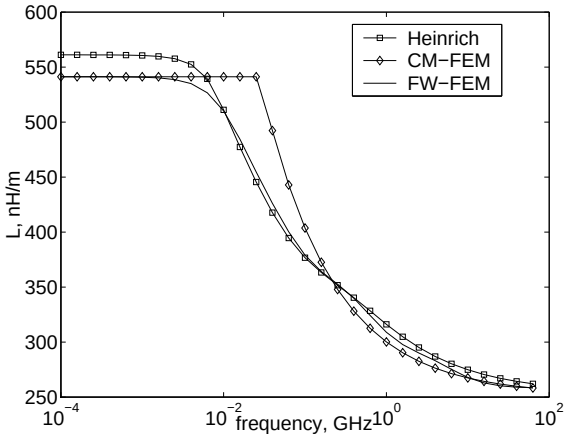

Figure 4: Total inductance of a rectangular CPW computed with the analytical model proposed in [7], the present approach, and FW-FEM.

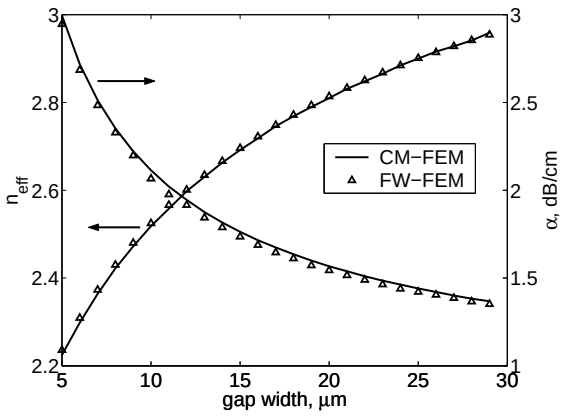

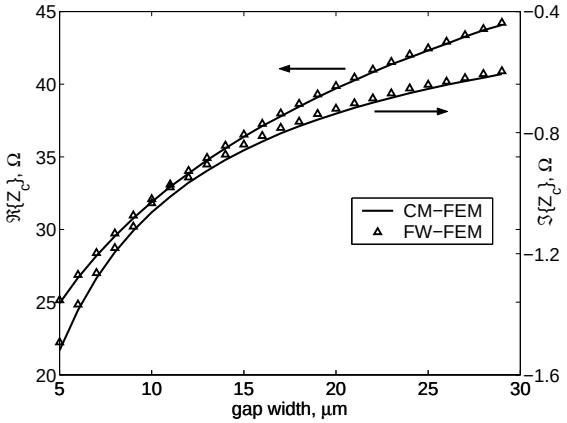

Figure 5: Microwave effective index n_{eff}, attenuation α (dB/cm), and characteristic impedance Z_c (Ω) of a rectangular CPW, computed with FW-FEM (triangles) and with the present approach (solid line) versus the width G of the gap between central electrode and ground planes.

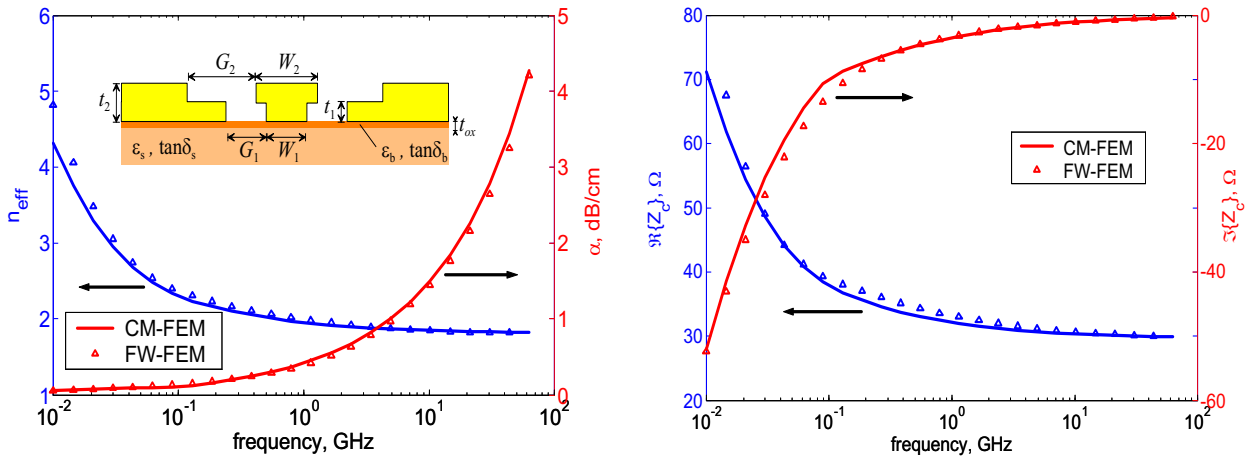

Figure 6: Microwave effective index n_{eff}, attenuation α (dB/cm), and characteristic impedance Z_c (Ω) of a mushroom CPW, computed with FW-FEM (triangles) and with the present approach (solid line) versus frequency.

effective index n_{eff}, the attenuation α (dB/cm), and the characteristic impedance Z_c (Ω) of the same rectangular line are shown as a function of the gap width G, as evaluated through the CM-FEM and the FW-FEM approaches at a frequency $f = 10\,\text{GHz}$. The excellent agreement demonstrates that the CM-FEM model provides an accurate estimate of the line parameters as a function of the line dimensions, and is therefore well suited for optimization. The same conclusions hold for more complex structures, like the mushroom CPW line ($\tan\delta_{\text{s}} = 0.004$, $\tan\delta_{\text{b}} = 0.016$, $t_{\text{ox}} = 1.1\,\mu$m, $t_1 = 15\,\mu$m, $t_2 = 25\,\mu$m, $W_1 = 7\,\mu$m, $W_2 = 16\,\mu$m, $G_1 = 12\,\mu$m, $G_2 = 18\,\mu$m) whose impedance, attenuation and effective permittivity are plotted in Fig. 6 versus frequency, as derived from the CM-FEM and FW-FEM approaches. Notice that typical CPU times for the CM-FEM approach are about one order of magnitude lower than for the FW-FEM method.
As a final remark, quasi-TEM models can be conveniently applied to capacitively loaded lines, like the one shown in Fig. 1, below. Such lines are exploited in semiconductor modulators for velocity matching purposes and cannot be easily analyzed through a 2D full-wave approach. On the other hand, the quasi-TEM technique allows for a simpler decomposition of the capacitance and leads to a more straightforward simulation of the C-loading effect.

Acknowledgment

This research was partially supported by CNR (Italian National Research Council) through the MADESS II project.

References

[1] G. Ghione, M. Goano, G. Madonna, G. Omegna, M. Pirola, S. Bosso, D. Frassati, and A. Perasso, "Microwave modeling and characterization of thick coplanar waveguides on oxide-coated lithium niobate substrates for electrooptical applications," *IEEE Trans. Microwave Theory Tech.*, vol. MTT-47, no. 12, pp. 2287–2293, Dec. 1999.

[2] M. Goano, F. Bertazzi, P. Caravelli, G. Ghione, and T. A. Driscoll, "A general conformal-mapping approach to the optimum electrode design of coplanar waveguides with arbitrary cross section," *IEEE Trans. Microwave Theory Tech.*, accepted for publication.

[3] F. Bertazzi, M. Goano, and G. Ghione, "Fast higher-order full-wave FEM analysis of traveling-wave optoelectronic devices," in *Proceedings of the 31st European Microwave Conference*, London, Sept. 2001, vol. 100, pp. ??–??

[4] M. Koshiba, *Optical Waveguide Theory by the Finite Elements Method*, KTK Scientific Publishers, Tokyo, 1992.

[5] T. A. Driscoll, "Algorithm 756: A MATLAB toolbox for Schwarz-Christoffel mapping," *ACM Trans. Math. Software*, vol. 22, no. 2, pp. 168–186, June 1996.

[6] T. A. Driscoll, *Schwarz-Christoffel Toolbox User's Guide. Version 2.1*, Department of Applied Mathematics, University of Colorado, Boulder, 1999.

[7] W. Heinrich, "Quasi-TEM description of MMIC coplanar lines including conductor-loss effects," *IEEE Trans. Microwave Theory Tech.*, vol. MTT-41, no. 1, pp. 45–52, Jan. 1993.